ELSEVIER

Journal of Power Sources 90 (2000) 214–223

JOURNAL OF POWER SOURCES

www.elsevier.com/locate/jpowsour

Simulation study of electrical dynamic characteristics of lithium-ion battery

Kiyonami Takano [a,*], Ken Nozaki [a], Yoshiyasu Saito [a], Akira Negishi [a], Ken Kato [a], Yoshio Yamaguchi [b]

[a] *Electrotechnical Laboratory, Energy Technology Division, Umezono 1-1-4 Tsukuba, Ibaraki 305-8568, Japan*
[b] *Chiba Institute of Technology, Narashino, Chiba 275-0016, Japan*

Received 11 August 1999; received in revised form 5 January 2000; accepted 19 February 2000

Abstract

The electrical dynamic characteristics of a lithium-ion battery have been simulated by an equivalent circuit, which is derived from the measured impedance. The transient voltage response to the various kinds of applied current waves such as single pulse, single rectangular, triangle, and sawtooth waves is experimentally examined and calculated by using the numerical Laplace transform with the equivalent circuit. The experimental and calculated results are compared and discussed, focusing on the range of current where the linear relationship is valid. Changing the time range, the state of charge (SOC) and the battery temperature as parameters, their influence on the linear range of the applied current has been investigated.

Keywords: Lithium-ion battery; Electrical characteristics; Equivalent circuit; Battery impedance; Nonlinear relationship; Laplace transform

1. Introduction

Lithium-ion batteries are widely used in many portable electronic devices, such as mobile telephones and laptop computers, because of their excellent performance, compact, high energy density, high reliability, etc. Lithium-ion batteries with a large capacity have been developed for application in electric vehicles, hybrid electric vehicles and load-leveling systems in homes. It is necessary for the electrical design of such application systems to understand the electrical characteristics of the lithium-ion battery. It is also useful to describe mathematically the characteristics for the efficient use of the battery.

In general, the electrical characteristics of batteries are based on the electrochemical reaction and the migration and diffusion of ions and chemical species during the charging and discharging processes, and they are very complex. Hence, it is difficult to precisely predict the dynamic voltage (or current) when an arbitrary wave current (or voltage) is applied to a battery. There are some methods to describe the current–voltage characteristics of batteries [1–3]. The linear circuit theorem is basic and it is useful to clarify the domain where the linear circuit theorem can be applied.

In this paper we attempt to describe the electrical characteristics of a lithium-ion battery with its equivalent circuit which is derived from the measured impedance. The transient voltage response to the various kinds of current waves applied to a commercial lithium-ion battery was experimentally examined and calculated by using the numerical Laplace transform [4] with the equivalent circuit. In the experiment, the magnitude of the applied current, the state of charge (SOC) and the battery temperature were the variables. The experimental and calculated results are compared and discussed for the range of current where a linear relationship is valid, including the influence of the time range, the SOC and the battery temperature.

2. Experiment

The battery used in these experiments is a commercial lithium-ion battery with capacity of 1250 mA h (US18650

* Corresponding author. Tel.: +81-298-61-5794; fax: +81-298-61-5805.
E-mail address: ktakano@etl.go.jp (K. Takano).

0378-7753/00/$ - see front matter
PII: S0378-7753(00)00413-4

in Sony battery pack NP-710) and is of a cylindrical type (diameter: 18 mm, height: 65 mm). The active electrode materials are $LiCoO_2$ in the positive electrode and a hard carbon in the negative. The electrolyte solution is a mixed solvent of propylene carbonate and diethyl carbonate with $LiPF_6$ as the supporting electrolyte. The PTC element devised in the battery was bypassed by making a short circuit in order to examine the characteristics without the PTC element. SOC = 100% is defined as the fully charged state with the 1*C* constant current followed by a 4.2 V constant voltage charging at 298 K, and SOC = 0% is defined as the discharged state with the 0.2*C* constant current discharging until 2.7 V at 298 K. Four batteries, with different SOC = 25%, 50%, 75% and 100%, were used to examine the influence of SOC. Their initial capacity is about 1296.2 mA h with a small scatter of 6.9 mA h (0.54%). An aluminum container housing the battery was set in a thermostated water bath, which was controlled to be at programmed temperature (273, 293, 298, and 323 K).

The battery impedance was measured to determine the equivalent circuit parameters using a potentio/galvanostat and a Fourier response analyzer (Solartron 1286/1255). The measurement was carried out in the galvanostat mode with a zero DC current and an applied sine wave current of 50 mA rms. Furthermore, in order to examine how the impedance changed with the amplitude of the applied current, it was measured using a digital recorder with an FFT analyzer (Yokogawa AR1100A) and a 100A potentio/galvanostat (Nikko NPGS10-100) with a function generator (NF 1915) that supplied the sine wave.

The voltage response was measured for the various current waves in the system shown in Fig. 1. The function generator (Hokutodenko HB-105) generates a programmed

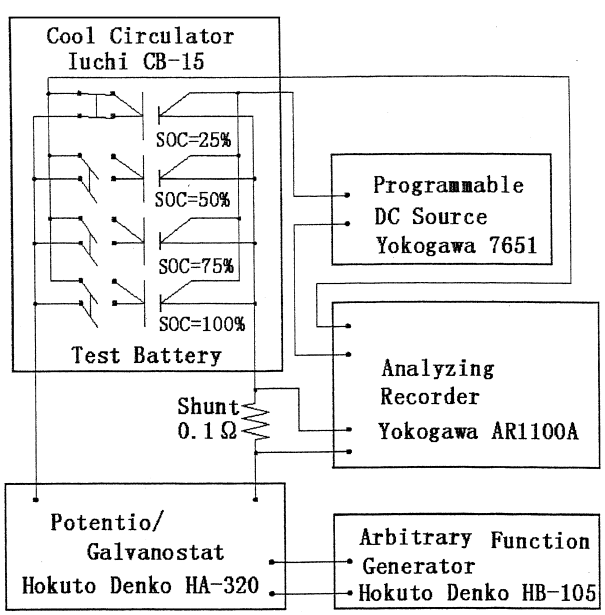

Fig. 1. Experimental system for voltage response measurement to various current waves applied to battery.

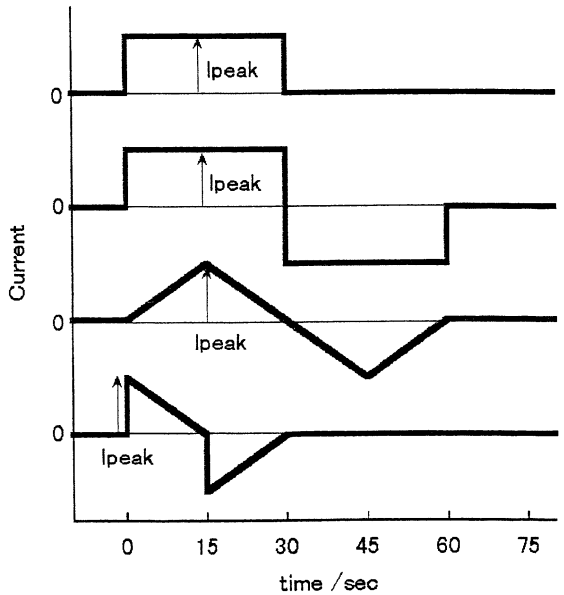

Fig. 2. Wave forms of applied current in voltage response measurements.

waveform signal to control the potentio/galvanostat (Hokutodenko HA-320) in the galvanostat mode. In order to measure the voltage response with high accuracy, the difference between the battery voltage and the DC bias voltage generated by the precise DC source (Yokogawa 7651) was measured with the digital recorder (Yokogawa AR1100A) as well as the current signal. The sampling rate is 2000 data points per second for the single pulse current, and 1000 data points per second for the other tests. The applied waveforms consisted of four kinds of single waves as shown in Fig. 2 and their reversed waves. A rest interval of about 30 min was taken at open circuit between the applied current.

3. Method of simulation

3.1. Simulation by the Laplace transform

The Laplace transform method is useful to analyze single waves or nonperiodic waves. The Laplace transforms, $I(s)$ and $V(s)$, of the current, $i(t)$, and the voltage response, $v(t)$, are given by the following equations [5]:

$$I(s) = \int_0^\infty i(t)e^{-st}dt = \int_0^\infty i(t)e^{-(\alpha+j\omega)t}dt \quad (1)$$

$$V(s) = \int_0^\infty v(t)e^{-st}dt = \int_0^\infty v(t)e^{-(\alpha+j\omega)t}dt \quad (2)$$

where the Laplace parameter, s:

$$s = \alpha + j\omega \quad (3)$$

where α is a positive real constant, ω is the angular frequency, j is an imaginary unit, and $j = \sqrt{-1}$. The value of α was given by the following equation as a

function of the analyzing period, T, for the numerical Laplace transform [4]:

$$\alpha = \frac{2\pi}{T} \tag{4}$$

The voltage response $v(t)$ to $i(t)$ is calculated by the inverse Laplace transform of $V(s)$ as follows:

$$v(t) = \int_{-\infty}^{\infty} V(s)e^{st}ds = \int_{-\infty}^{\infty} H(s)I(s)e^{st}ds \tag{5}$$

where $H(s)$ is the Laplace transfer function that is defined as:

$$H(s) = \frac{V(s)}{I(s)} \tag{6}$$

The Laplace transfer function of the battery, $H(s)$, can be calculated based on the linear circuit theorem from its equivalent circuit derived from the measured impedance for a range of frequencies.

The calculation of Eqs. (1) and (5) were carried out using the numerical Laplace transformation and inversion with the FFT algorithm [4] for 2048 discrete sample points.

3.2. Battery impedance and equivalent circuit

The Bode diagram and Cole–Cole plot of the measured impedance of a lithium-ion battery with 50% SOC are shown in Figs. 3 and 4, respectively. The frequency range is from 1 to 10 kHz. The impedance changes with the temperature and the SOC. However, in the range of 25–100% SOC, in which the experiment was conducted, the impedance change due to the SOC was relatively small.

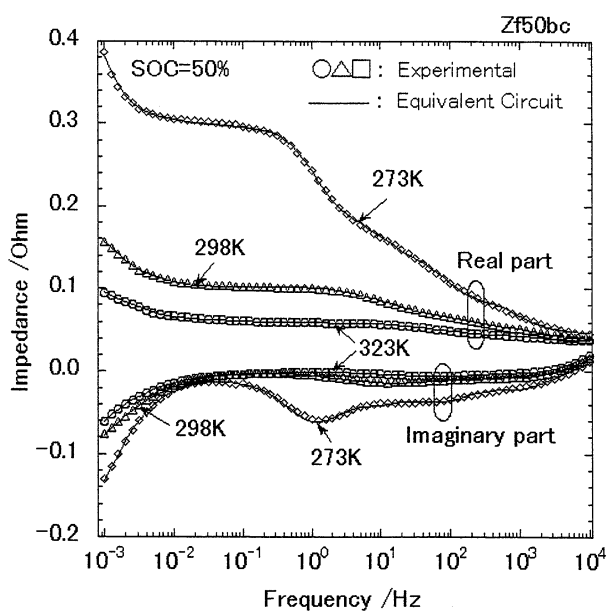

Fig. 3. Bode diagrams for measured impedance and calculated impedance using equivalent circuits for a lithium-ion battery with 50% SOC.

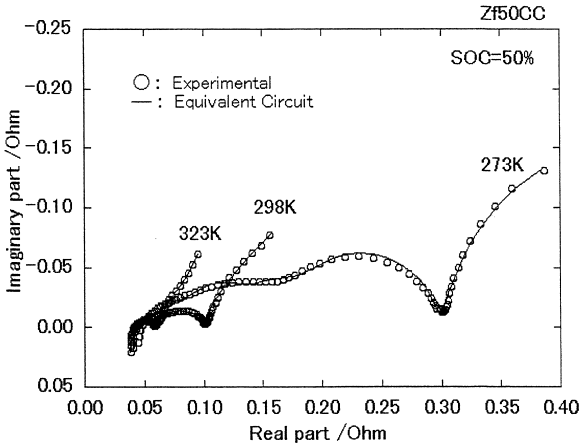

Fig. 4. Cole–Cole plots for measured impedance and calculated impedance using equivalent circuits for a lithium-ion battery with 50% SOC.

Before and after the experiment on the voltage response, the battery impedance was measured and a small impedance change was observed. Although the maximum change was about 3% at 298 and 323 K, at a low temperature, 273 K, it was 20% at low frequency. The impedance at 273 K clearly decreased after the experiment. The average values of the measured impedance were used in the simulation.

It was found through trial and error that the equivalent circuit shown in Fig. 5 could well represent to the impedance of the tested lithium-ion batteries. The Z_W in Fig. 5 is the Warburg impedance. The values of the parameters in the equivalent circuit were determined by numerically fitting to the measured impedance to minimize root mean square error. Although we cannot concretely determine the physical meaning of each element in the equivalent circuit by numerically fitting, we suppose the following. L_0 is owing to the inductance of spirally wound electrodes. R_0 is summation of the resistances of electrode tabs, electrode collectors, electronic resistance of electrode materials and ionic resistance of electrolyte. Parallel circuits of R and C are owing to resistance and capacity of the solid electrolyte interphase (SEI) that covers electrode surfaces, and reaction resistance and double layer capacitance of electrodes. The parallel circuit of R_5 with Z_W in series and C_5 means the reaction resistance and double layer capacitance of the positive or negative electrode that is affected by diffusion. In the case that both positive and negative electrodes are affected by diffusion, the effects of both are effectively accounted of only in Z_W. The number

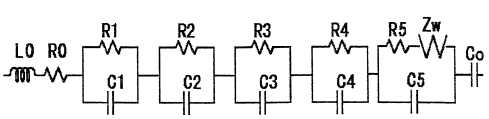

Fig. 5. Equivalent circuit applied in the electrical-characteristics simulation of a lithium-ion battery. Z_W is the Warburg impedance described in Eq. (7).

Table 1
Values of parameters in equivalent circuit for test conditions

T (K)	298				293	273	323
SOC	100%	75%	50%	25%	100%	50%	50%
L_0 (μH)	0.31875	0.31263	0.31974	0.33056	0.31103	0.2576	0.34575
R_0 (mΩ)	39.25	39.49	40.016	39.626	40.547	47.161	38.06
C_0 (F)	$>10^{10}$	$>10^{10}$	$>10^{10}$	2279.3	$>10^{10}$	$>10^{10}$	5565.4
R_1 (mΩ)	14.38	16.87	14.983	14.213	16.911	35.629	5.96
R_1C_1 (ms)	0.09165	0.12055	0.09055	0.07595	0.16032	0.14128	0.08928
R_2 (mΩ)	13.82	17.621	14.013	11.836	15.926	55.347	8.1
R_2C_2 (ms)	1.0931	2.0399	1.0203	0.6096	1.6574	1.8657	1.2847
R_3 (mΩ)	22.34	23.871	21.539	15.252	30.87	44.046	6.52
R_3C_3 (ms)	10.275	19.443	9.5422	4.693	16.933	14.6	8.3012
R_4 (mΩ)	11.45	3.3922	11.185	39.573	36.576	232.94	3.98
R_4C_4 (s)	0.05575	0.8269	0.05359	80.068	0.07321	272.03	1.590
R_5 (mΩ)	34.632	51.87	33.547	19.137	80.309	112.17	26.468
R_5C_5 (s)	29.431	48.748	23.250	0.02565	75.616	0.14405	33.355
σ_W (mΩ rad$^{-0.5}$)	7.6707	5.8816	8.70	2.9673	7.1091	3.3687	2.8657
Fitting error	0.96 %	0.85 %	0.98 %	1.01 %	0.97 %	1.03 %	0.58 %

of parallel circuits was added up to five in order to minimize the fitting error, considering the complex parallel distributions of electrode reactions in the electrodes in parallel. C_0 is used to take account of change in the electromotive force by the SOC.

The fitting values of the parameters in the equivalent circuit for each test condition are shown in Table 1 together with fitting errors. The calculated impedance from the equivalent circuit is also shown in Figs. 3 and 4, compared with the experimental data. The difference between the calculated and the experimental is only about 1%, and the equivalent circuit of Fig. 5 is a good model for discussing about the relation between voltage response and current. However, the dependence of each obtained parameter to SOC and temperature is complicated and it cannot be denied that there is a better equivalent circuit. We will discuss this problem in other paper.

The Warburg impedance Z_W is mathematically described as:

$$Z_W = \frac{\sigma_W}{\sqrt{2\omega}}(1-j) \tag{7}$$

where σ_W is a positive constant. The Laplace transfer function of the Warburg impedance, $H_W(s)$, is assumed as in Eq. (8), which is derived from the analytic continuation of Eq. (7).

$$H_W(s) = \frac{\sigma_W}{\sqrt{s}} \tag{8}$$

4. Results and discussion

4.1. Influence of the current magnitude

The experimental and calculated voltage responses to a single pulse current applied to a battery with a 100% SOC at 293 K are shown in Fig. 6. The applied peak current was changed from $0.2C$ (0.25 A) to $10C$ (12.5 A) in both direction of discharge (+) and charge (−) as a parameter. The number of experimental points plotted was reduced to simplify the plot. There is a good agreement between the experimental and the calculated data at the small peak current in both directions of discharge and charge below $1C$ (1.25 A). The difference between the experimental and the calculated data increases with the peak current in both directions when over $2C$ (2.5 A).

It is speculated that one of the causes of the difference for the large current comes from the nonlinear relationship of the charge transfer reactions in the battery. The relation between reaction current i and overpotential η in a charge-transfer electrode reaction on an electrode surface is described by the following equation [6]:

$$i = i_0\left\{\frac{C_0(0,t)}{C_0^*}\mathrm{e}^{\frac{\alpha nF}{RT}\eta} - \frac{C_R(0,t)}{C_R^*}\mathrm{e}^{\frac{(1-\alpha)nF}{RT}\eta}\right\} \tag{9}$$

where i_0 is the exchange current; $C_0(0,t)$ and $C_R(0,t)$ are concentrations on electrode surface of Ox and Re, respectively, in the electrode reaction Eq. (10); C_0^*, C_R^* are bulk concentrations of Ox and Re, respectively; α is the transfer coefficient; n is the number of electrons per molecule oxidized or reduced; F is the Faraday constant; R is the gas constant; t is time; and T is temperature:

$$\mathrm{Ox} + ne \rightleftarrows \mathrm{Re} \tag{10}$$

The concentrations on the surface are equal to the bulk concentrations, if there is no effect of the mass transfer, and Eq. (9) becomes:

$$i = i_0\left\{\mathrm{e}^{-\frac{\alpha nF}{RT}\eta} - \mathrm{e}^{\frac{(1-\alpha)nF}{RT}\eta}\right\} \tag{11}$$

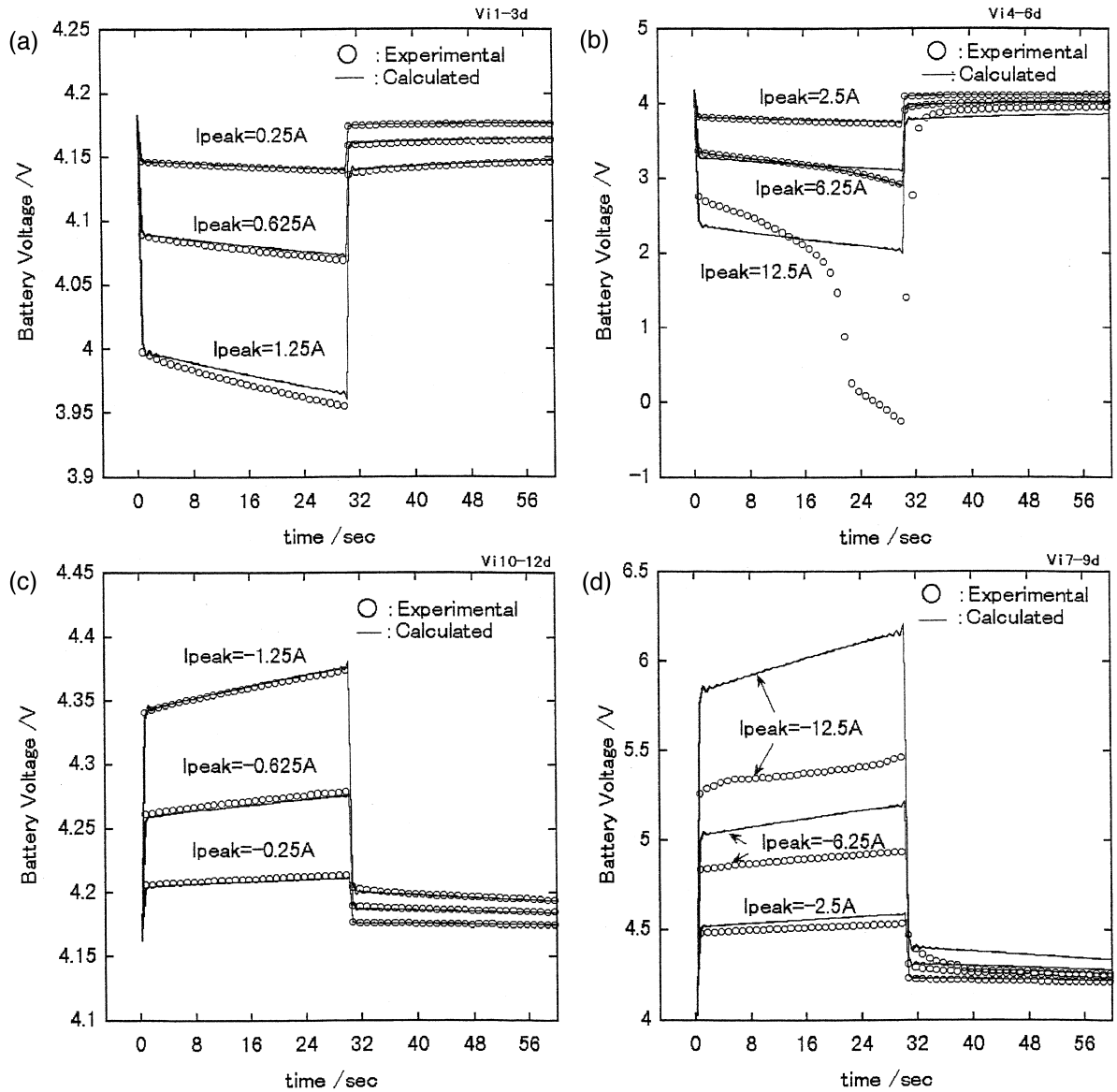

Fig. 6. Comparison between experiment and simulation in a voltage response to single pulse current applied to a lithium-ion battery with 100% SOC at 293 K (parameter: peak current of pulse). (a) Discharge of 0.25 to 2.5 A. (b) Discharge of 2.5 to 12.5 A. (c) Charge of 0.25 to 2.5 A. (d) Charge of 2.5 to 12.5 A.

Thus, charge transfer current is an exponential function of the overpotential η, and the effective reaction resistance decreases for a large overpotential at the large current.

The battery impedance measured by applying a sine wave is shown in Fig. 7 as a function of the peak-to-peak amplitude (Ap–p) of the current. The data in these figures are restricted for the frequency range where the duration for the measurement is short to prevent temperature rising. These figures support the above-mentioned speculation. That is, the impedance–current curve has a plateau and the impedance decreases with an increase in the current over the knee point as shown in Fig. 7(a). The current of the knee point decreases with frequency and it is about 2 Ap–p at 0.1 Hz. The Cole–Cole plots in Fig. 7(b) indicate decrease in the radius of semi-circles that may be corresponded to the reaction resistance or the SEI's resistance below 2 Ap–p. Although electrical characteristic of SEI is not well yet understood, there may be a nonlinear relation between current and voltage, if there are SEI's growth and elution by discharge and charge.

It is considered that the temperature rise is one of the causes of the decrease of voltage drop in large current. However, the temperature rise after 30 s is estimated at most even in 6.25 A case with about 5 K at adiabatic condition, and its effect seems to be rather small. It is supported by the another reason that the difference of calculation and experiment has also already appeared after 1 s.

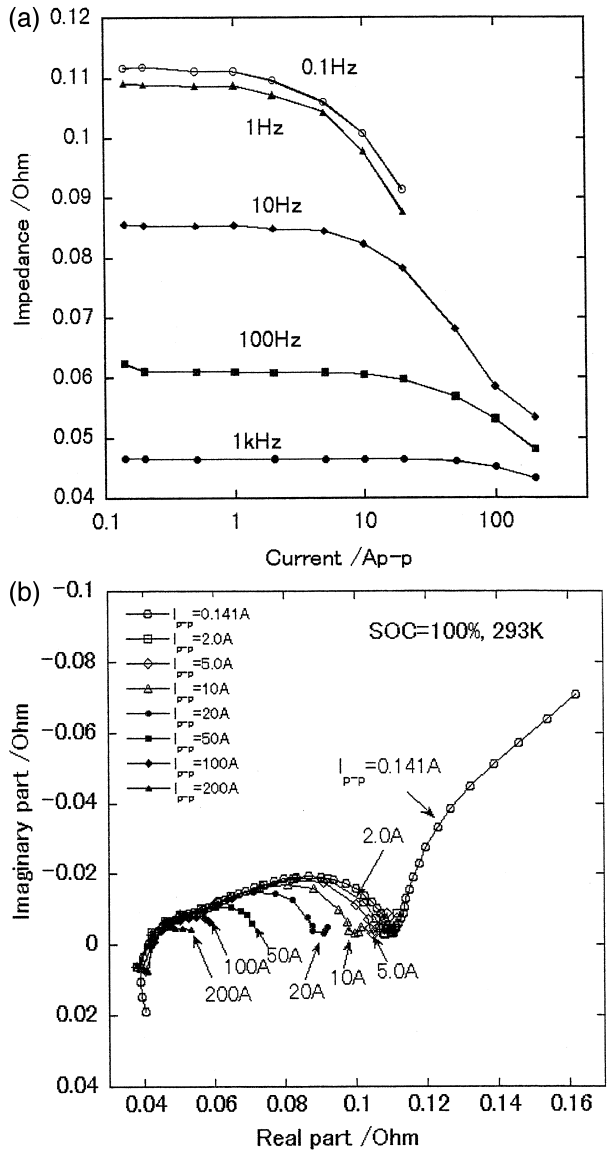

Fig. 7. Variations in measured impedance due to amplitude of applied sine wave current in a lithium-ion battery with 100% SOC at 293 K. (a) Absolute values of impedance vs. peak-to-peak current. (b) Cole–Cole plots.

Because it is considered that side reactions such as the decomposition of electrolyte besides the charging reaction occur when the charging voltage exceeds 4.5 V, the experiment voltage lowers from the calculated one.

The experimental voltage drop for higher current discharges above 6.25 A becomes greater than the calculated one after 20 s as shown in Fig. 6(b). This difference may be caused by another factor. In our model, mass transfer effect is accounted by the Warburg impedance, Z_W, which is valid in the limitless diffusion. However, at a large current the bulk concentration changes in a period due to mass transfer. From a simulation study [7], it is speculated that the charge transfer at a large discharge current may cause a reduced region of lithium ions in the electrolyte in the porous positive electrode, and thus the diffusion of lithium ion may limit the current, resulting in a large voltage drop. And, it is also speculated that voltage drop may increase via diffusion limitation of lithium ion in cathode-active material ($LiCoO_2$) in the large current. By the diffusion limitation, lithium concentration of the positive electrode surface rapidly increases in the large current, and the positive electrode potential rapidly lowers. The current after 22 s at 12.5 A in Fig. 6(b) may be transferred through lithium metal plating on the surface with a battery voltage below 0 V. It is guessed that the increase of the voltage drop by diffusion limitation in negative electrode may occur by the conditions of SOC and so on.

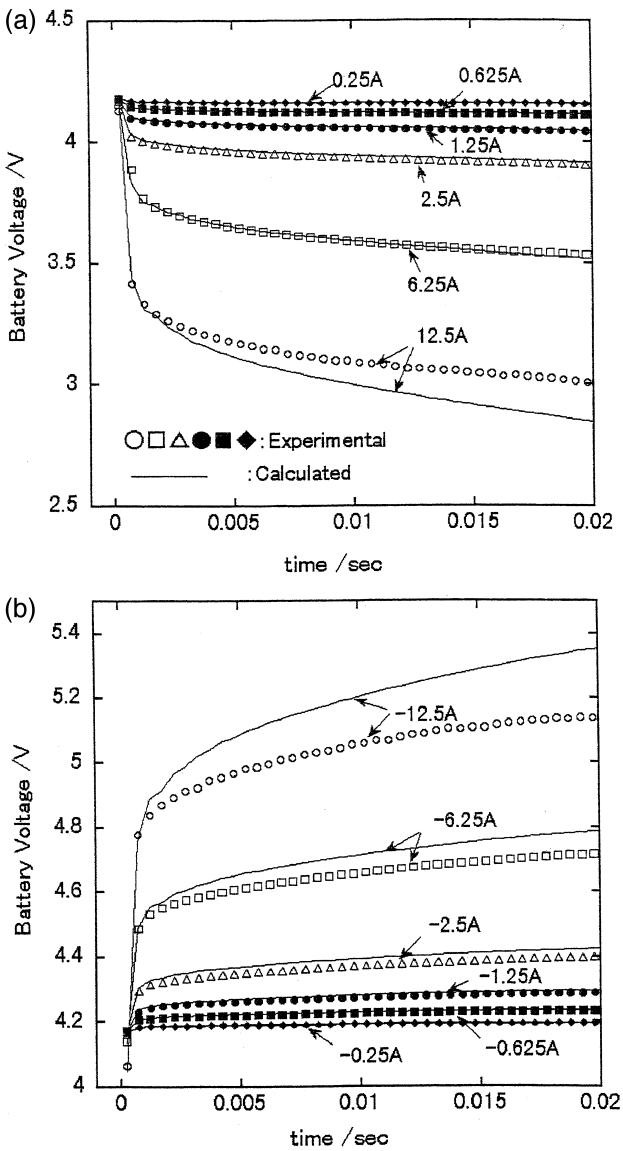

Fig. 8. Comparison between experiment and simulation in initial voltage response to single pulse currents applied to a lithium-ion battery with 100% SOC at 293 K. (a) Discharge. (b) Charge.

While in the charge direction, the experimental voltage drop is less than the calculated one even if it is 12.5 A, as shown in Fig. 6(d). It is speculated that the diffusion limitations do not occur in the both electrodes even if 12.5 A charges. These results show that the linear region of the current looks wider during discharge than during charge.

4.2. Influence of the time range

To examine the influence of the time range, the voltage responses for the initial 20 ms of the applied pulse shown in Fig. 6 are closed in Fig. 8. The short time response within the initial few milliseconds indicates a good agreement between the experimental and the calculated data even for a 10*C* (12.5 A) discharge. While in the longer time range, the experimental response to the smaller current shifts from the calculated one. That is, for the shorter time range, the larger current maintains a linear relationship between current and voltage responses. This corresponds to the fact that the impedance does not change for a higher frequency until a larger current is applied, as shown in Fig. 7(a). According to the equivalent circuit, this is explained as follows. At the higher frequency, the nonlinearity of the charge transfer reaction (or SEI's resistance) is masked by bypassing through the double layer capacitance (or SEI's capacitance), which is in parallel with the reaction (or SEI) resistance.

4.3. Influence of the temperature

Fig. 9 shows the voltage responses to a single rectangular wave of current applied to the battery with 50% SOC at three different temperatures, 273, 298, and 323 K. In the rectangular wave, there is also a good agreement between the experimental and the calculated data at small currents similar to the single pulse and their difference increases with the current.

The temperature of the batteries affects the linear range of the current. At higher temperatures, the higher current maintains a good agreement between the experimental and the calculated results, as shown in Fig. 9. That is, the increase in the temperature expands the linear range of the current. The reason why the increase of the temperature expands the linear range of the current is speculated as follows.

Taking notice of 273 K in which the nonlinearity has remarkably appeared as shown in Fig. 9(a), the voltage drop of the experiment is smaller than the calculation, and

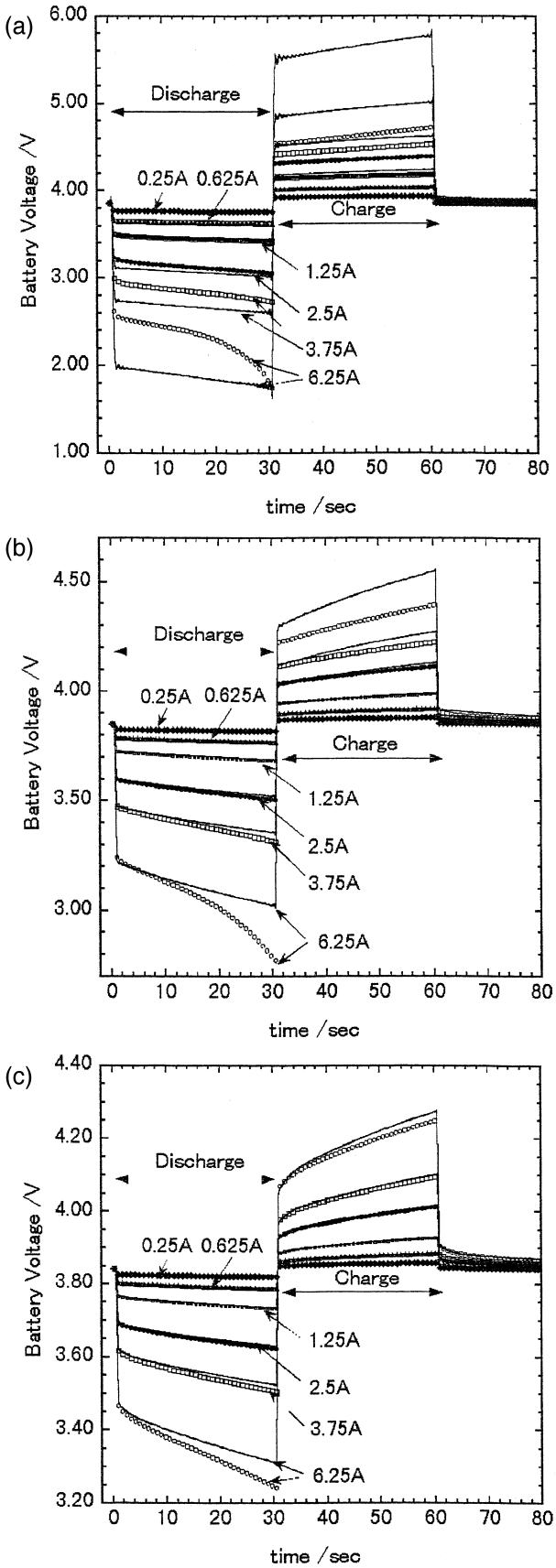

Fig. 9. Comparison between experiment (symbols) and simulation (lines) in voltage response to single rectangular wave of current applied to a lithium-ion battery with 50% SOC. (a) At 273 K. (b) At 298 K. (c) At 323 K.

the difference drastically increases with the increase in the current over 2.5 A. While taking notice of the impedance used in the calculation, resistance components in *RC* parallel circuits drastically increase by lowering temperature from 298 to 273 K as shown in Fig. 4 and Table 1. In short, the drastic increase of reaction resistances and/or SEI's resistances occurs at 273 K and it brings the large voltage drop in the calculation. Therefore, we guess that the reason why the voltage drop of the experiment becomes much smaller than the calculated one seems to be caused by the decrease in reaction resistances and/or SEI's resistances by the current increase. It is considered that the exchange current decreases on the increase of the reaction resistance at a reduced temperature, because the reaction resistance R_{ct} for small overpotential is given by the following equation [6]:

$$R_{ct} = \frac{RT}{nFi_0} \quad (12)$$

According to Eq. (11), the decrease of the exchange current means the decrease in the current range where linear approximation is valid. Thus, the decrease of the temperature may narrow the linear range of the current, while the change of SEI's resistance by discharge and charge is also supported by an evidence that the decrease in the impedance was observed after the tests, as mentioned in Section 3.2, and it is suggested that there are nonlinear characteristics in SEI.

In the comparison between the discharging part and the charging part in a rectangular wave in Fig. 9, the experimental voltage drop during discharging is larger than that during charging, which is the same as the case of the single pulse response. The same results were also obtained for the reversed rectangular wave of current.

4.4. Influence of the SOC

The voltage responses to the rectangular wave for the different SOC, 25%, 75%, and 100% at 298 K, are shown in Fig. 10. At these SOCs, differences due to the SOC in the linear range of current cannot be clearly found. However, it is remarkable that the experimental run of 5*C* (6.25 A), at the SOC of 25%, significantly shifts from the calculated one compared with the results at the other SOCs. This suggests that the nonlinearity of the voltage response may become larger at much lower SOCs because, since the reaction site in the electrode active materials decreases in deep discharge and the limiting current decreases, then the linear region narrows.

4.5. Influence of the wave form

Fig. 11 shows the voltage responses to the single triangle wave and the single sawtooth waves of applied current in a battery with 50% SOC at 298 K. The linear relation-

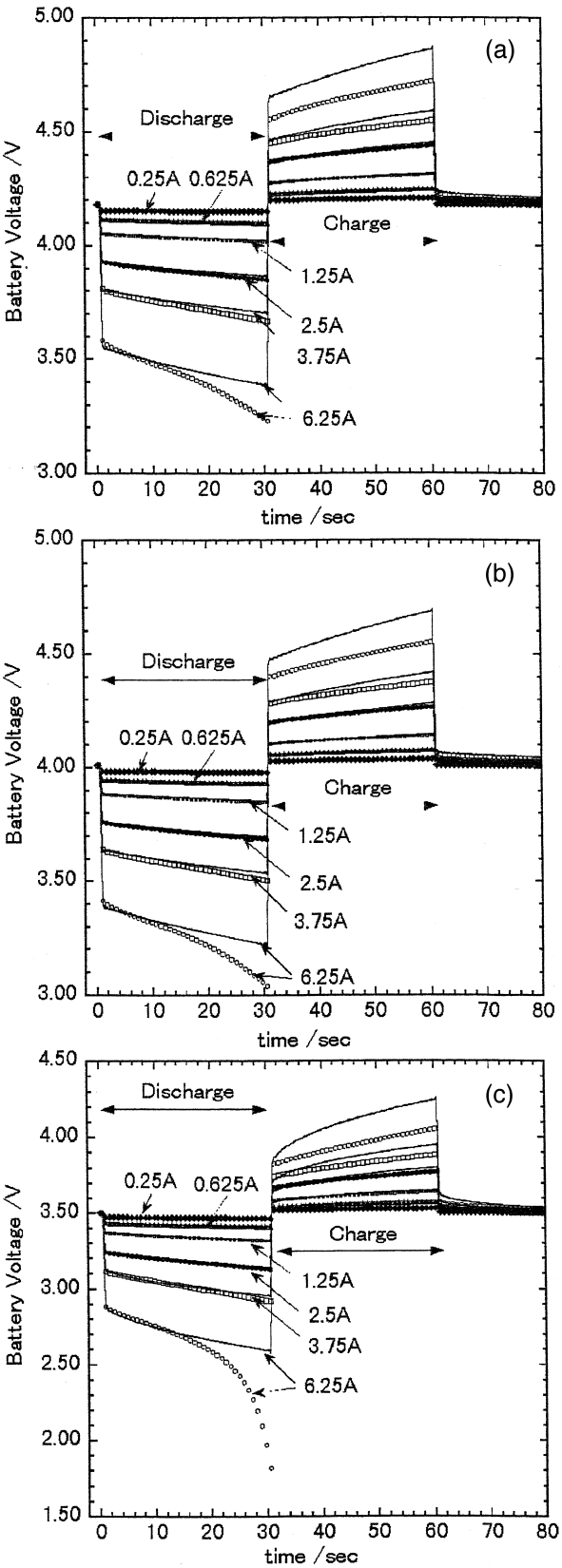

Fig. 10. Comparison between experiment (symbols) and simulation (lines) in voltage response to single rectangular waves of current applied to lithium-ion batteries with different state of charge at 298 K. (a) SOC = 100%. (b) SOC = 75%. (c) SOC = 25%.

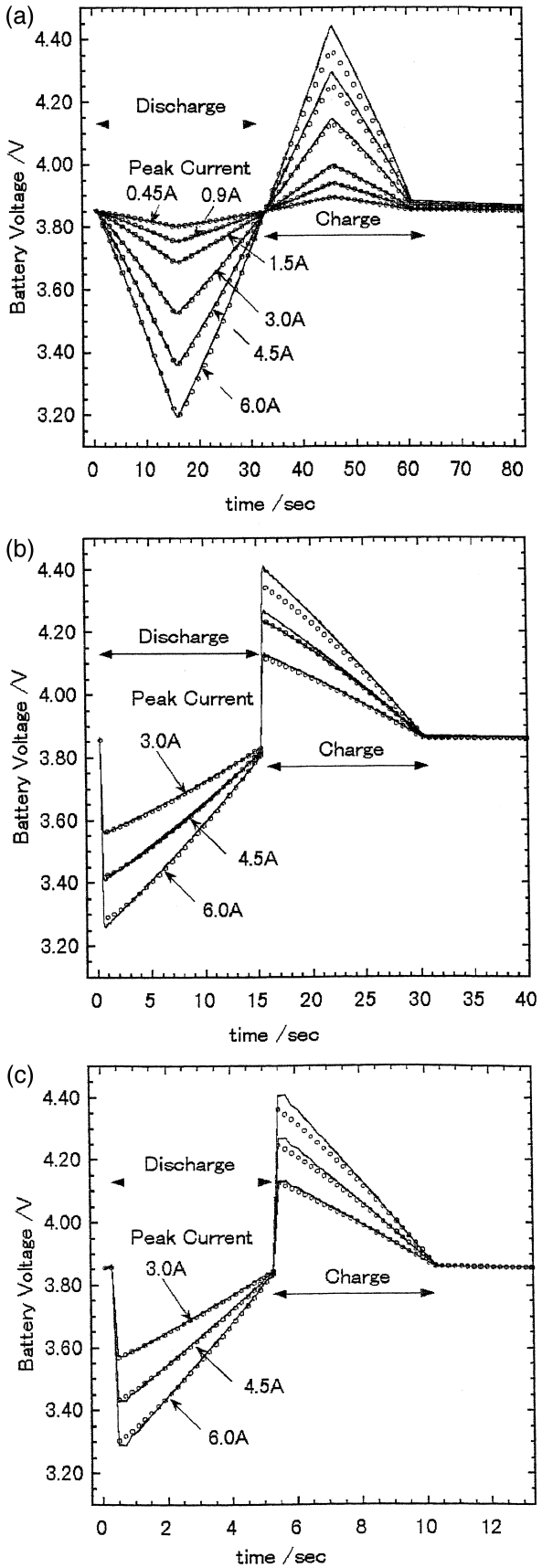

Fig. 11. Comparison between experiment and simulation of voltage response to single various waves of current applied to a lithium-ion battery with 50% SOC at 298 K. (a) Triangle wave. (b) Sawtooth wave (1). (c) Sawtooth wave (2).

ships of the voltage responses to both waves are not qualitatively different from the results of the other waves mentioned above. However, the experimental results for the triangle or sawtooth waves agree with the calculated data for the higher peak currents as compared to for the rectangular wave. The reason is speculated because the total mass transfer quantity until the current reaches a peak value in the triangle or sawtooth waves is smaller than in the rectangular wave if peak values are the same. Besides, effects of the no faradic current is small in a time range over 1 s.

5. Conclusions

The transient voltage response to the various kinds of the current wave applied to a commercial lithium-ion battery has been experimentally examined and calculated by using the numerical Laplace transform with the equivalent circuit derived from the impedance that is measured by small sine-wave currents. From the comparison and the discussion, a number of things have been clarified.

(1) There is a good agreement between the experimental and the calculated voltage responses for every wave shape of a small current magnitude. As the current increases over a certain value, the nonlinearity of the voltage response appears and the experimental data differs from the calculated data.

(2) The range of current that maintains the linear relationship in voltage response depends on the time range, the temperature and the direction of current flow. In the short time range of a few milliseconds, the linear range of current expands and the linear relationship can be supposed up to the peak current rate of 10C during discharge. Also the linear range expands with temperature. Further, it is wider in discharge than in charge. For example, in the range of 30 s, the linear relationship of the voltage response can be observed up to the peak current rate of 2C discharging for the pulse or the rectangular wave in the tested lithium-ion battery with 100% SOC at 293 K.

(3) The linear range of the current hardly changes with the SOC between 25% and 100%. However, it was suggested from the results at SOC = 25% that the linear range became narrow with a decreased SOC below 25%.

(4) The linear relationship of the voltage response was qualitatively the same among the various tested wave shapes of current. However, the experimental data for the triangle wave agrees with the calculated one for higher current peaks than for the rectangular wave.

(5) The above-mentioned results correspond well to the relationship between the applied current amplitude and the impedance measured by applying a sine wave.

References

[1] T.C. Leisgang, A.J. Johnson, D.P. Hafen, Dynamic performance battery model, Proceedings of 23rd IECEC 889465 (1988) 439.
[2] D. Mayer, S. Biscaglia, Modeling and analysis, Proceedings of 9th Conference on Photovoltaic Solar Energy,1989, p. 245.
[3] K. Sawai, T. Ohzuku, A method of impedance spectroscopy for predicting the dynamic behavior of electrochemical system and its application to a high-area carbon electrode, J. Electrochem. Soc. 144 (1997) 988.
[4] D.J. Wilcox, Numerical Laplace transformation and inversion, Int. J. Elect. Eng. Educ. 15 (1978) 247.
[5] A. Poularikas, The Transforms and Applications Handbook, CRC Press, Boca Raton, 1996.
[6] A.J. Bard, L.R. Faulkner, Electrochemical Methods, Fundamental and Applications, Wiley, New York, 1980, p. 103.
[7] T.F. Fuller, M. Doyle, J. Newman, Simulation and optimization of the dual lithium ion insertion cell, J. Electrochem. Soc. 141 (1994) 1.